Wideband 4-Port MIMO Antenna Array for 5G Millimeter-Wave Mobile Device Terminals

Nathapat Supreeyatitikul* (1), Phanuphong Boontamchauy (2)
(1), (2) Aeronautical Engineering Division, Civil Aviation Training Center of Thailand
1032/355 Phaholyothin Road., Jatujak, Bangkok 10900, Thailand

Abstract

A multiple-input multiple-output (MIMO) antenna system is proposed for fifth-generation (5G) millimeter-wave (mm-wave) mobile communications. The proposed design provides a wide bandwidth at the mm-wave frequency of 24 GHz to 40 GHz ($S_{11} \leq$ -10 dB) with high isolation (S_{12} > 40 dB) that achieved by a T-shaped radiating patch with a slot-based on the ground plane. An integrated four-element MIMO antenna has an overall size of 150×75×0.2 mm^3. Moreover, the proposed MIMO has been investigated for the performance diversity, in terms of the envelope correlation coefficient and diversity gain, which has a good agreement that appropriates for mobile terminals applications.

1 Introduction

Multiple-input multiple-output (MIMO) antenna [1] is attractive from the researcher for fifth-generation (5G) wireless communications [2]. MIMO has been achieved by the high data rate and wide bandwidth provided for enormous usage at the same time. The spectrum of 5G new radio (NR) technologies [3] can be classified into three categories such that low-band (below 1 GHz), mid-band (sub-6 GHz), and high-band (above 24 GHz, also known as mm-Wave). The global usually operate a licensed millimeter-wave spectrum in various frequency ranges [4], such as 24.25 - 25.25 GHz in America, 27.5 - 28.35 in Canada, 24.5 - 28.35 GHz in Europe, 26 GHz in UK, 24.5 - 27.5 GHz in China, 26.5 - 29.5 GHz in Korea, and 27.5 - 29.5 GHz in Japan.

In this paper, an integrated four-element 5G mm-wave MIMO antenna system that operated the wideband frequency of 24 GHz to 40 GHz for mobile devices. Furthermore, a proposed MIMO antenna has been presented and its performance diversity is calculated and discussed. The proposed antenna design is presented in Section II. Then, Section III describes the result and discussion. After that, the conclusion is given in Section IV.

2 Antenna Design

The proposed wideband MIMO slot-based antenna array has been shown in Figure 1. The proposed design consists of four antenna elements printed on Rogers RO4003C with a dielectric constant (ε_r) of 3.55, loss tangent (δ) of 0.0027 and a height of 0.2 mm. The single element antenna employed proximity fed by a 50Ω microstrip feed line as a T-shaped radiating patch that placed above the substrate and etched a rectangular-shaped slot on the ground plane, while each antenna element size of 6×10 mm^2. The overall size of the integrated MIMO antenna is 150×75×0.2 mm^3. The proposed MIMO antenna system was assembled of two adjacent antenna elements were symmetrically arranged along the vertical edge of the mobile on both sides, which a distance of 5λ (53.5 mm) at the center frequency of 28 GHz.

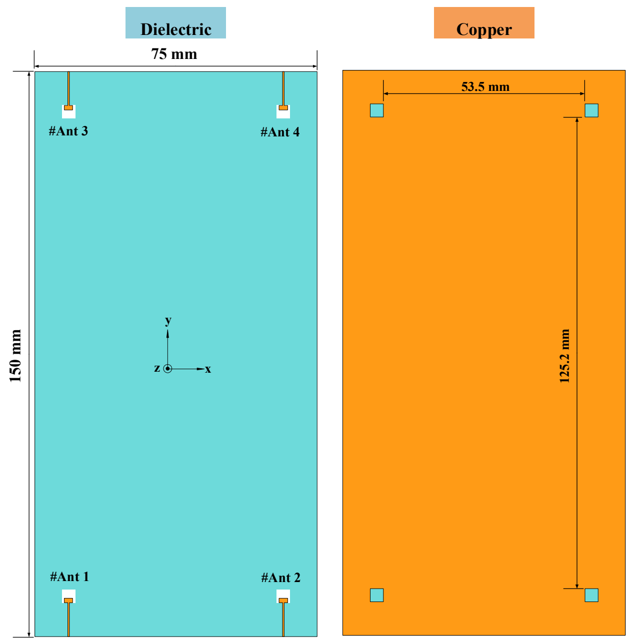

(a) Top view (b) Bottom view

Figure 1. The proposed MIMO antenna system.

3 Result and Discussion

The simulation was performed by using CST Microwave Studio Simulation. Some metrics that important to the conventional performance of the antenna, which include of the reflection coefficient, transmission coefficient (mutual coupling), and radiation pattern. In addition, in order to investigate the diversity performance of the MIMO antenna systems such that the envelope correlation coefficient (ECC) and diversity gain (DG).

3.1 Reflection coefficient

The simulated reflection coefficient (S_{11}, S_{22}, S_{33}, and S_{44}) obtained that the -10dB bandwidth was 16.50 GHz from 24.10 GHz to 40.60 GHz, as shown in Figure 2. Figure 3 shows the simulated transmission coefficient (S_{12}, S_{13}, S_{23}, and S_{34}) of two-port is lower than -40 dB over the entire band that appropriates for the four-port MIMO antenna system applied in mobile terminals.

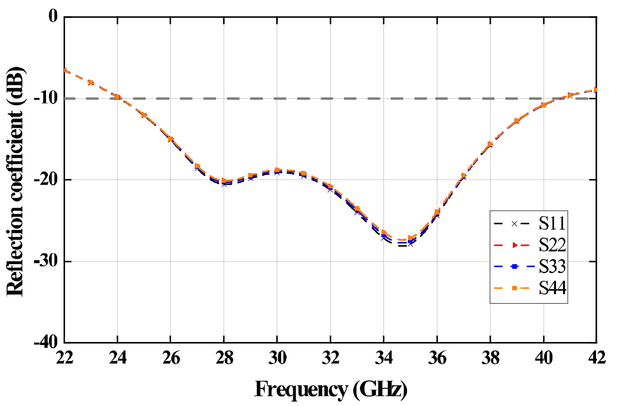

Figure 2. The simulated reflection coefficient.

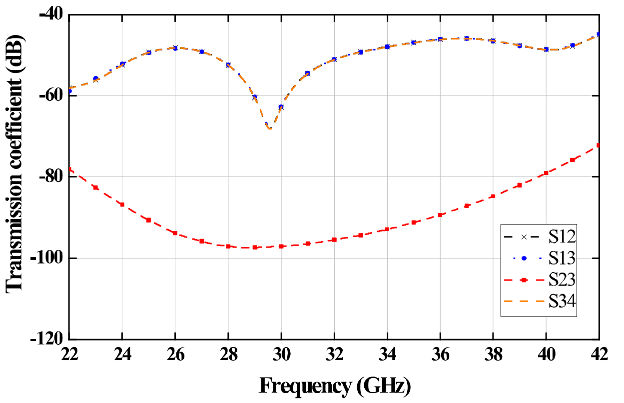

Figure 3. The simulated transmission coefficient.

3.2 ECC and DG

The Envelope correlation coefficient (ECC) is the parameter that indicates the correlation between the radiating antenna elements. It is calculated based on the far-field radiation patterns between antenna pairs at the operating entire frequency, using the following equation [5].

$$ECC = |\rho_{12}|^2 = \frac{\left|\iint_{4\pi}[E_1(\theta,\phi) * E_2(\theta,\phi)]\right|^2}{\iint_{4\pi}|E_1(\theta,\phi)|^2\, d\Omega \iint_{4\pi}|E_2(\theta,\phi)|^2\, d\Omega} \quad (1)$$

where $E_1(\theta,\phi)$ and $E_2(\theta,\phi)$ are the complex 3D radiated field pattern of Ant 1 and Ant 2, respectively and Ω is the solid angle. Figure 4 reveals the ECC has lower than 0.001 of them between the antenna pairs at the overall operating frequency, it is noted that the ECC threshold should less than 0.5 [6].

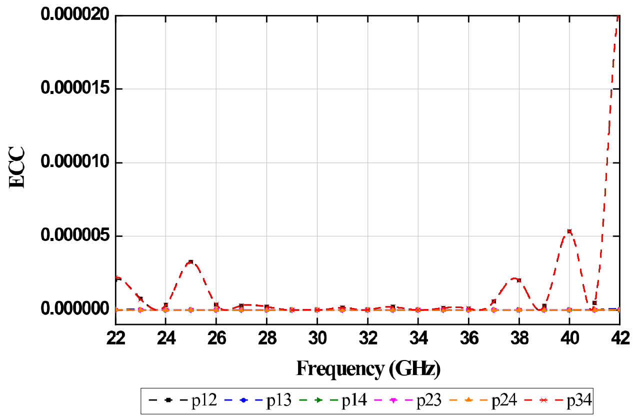

Figure 4. The calculated envelope correlation coefficient.

Meanwhile, diversity gain (DG) is one important parameter to clarify how much transmission power can be reduced when a diversity scheme is introduced, without a performance loss. DG can be computed by using ECC values, following by equation [7].

$$DG = 10\sqrt{1-|\rho_{12}|^2} \quad (2)$$

As it is shown in Figure 5, the calculated diversity gain is plotted versus over the entire frequency (24 GHz – 40 GHz). It is demonstrated that the DG greater than 9.99 dB, which notices that DG should exceed 9.95 dB [8].

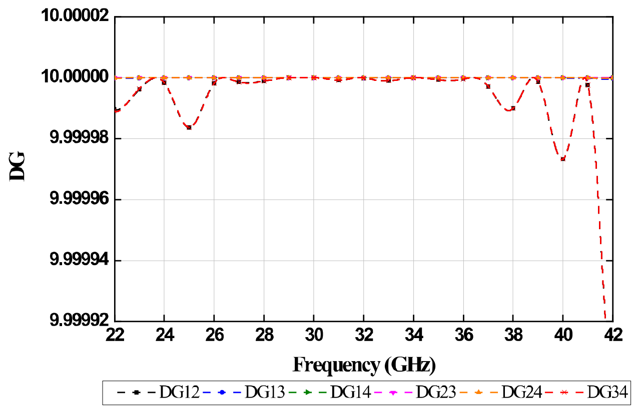

Figure 5. The calculated diversity gain.

3.3 Radiation pattern

Figures 6 illustrate the 3D radiation pattern in the form of the directivity at a frequency of 28 GHz. It can be observed that the maximum gains of 4.48, 4.89, 4.49, and 4.51 dBi for Ant 1 to Ant 4, respectively.

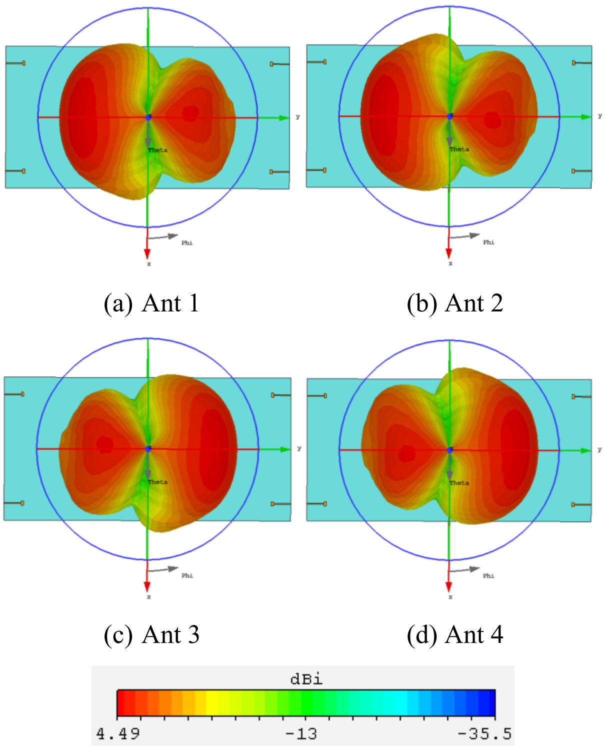

(a) Ant 1 (b) Ant 2

(c) Ant 3 (d) Ant 4

Figure 6. 3D radiation patterns for the antenna elements with directivity values at 28 GHz.

4 Conclusion

A four-port MIMO antenna array for millimeter-wave mobile terminal applications is proposed. Compact size is achieved by a T-shaped as a radiating patch with a slot-based on the ground plane. The MIMO antenna obtained a wide bandwidth frequency of 24 GHz to 40 GHz $(\leq -10\,dB)$. The port isolations are better than 40 dB, the calculated ECCs lower than 0.001 and the calculated DGs are not less than 9.99 dB. Therefore, the proposed MIMO antenna array has a good performance that suitable for millimeter-wave mobile devices applications.

5 References

1. Dirk Manteuffel, “MIMO antenna design challenges,” *2009 Loughborough Antennas & Propagation Conference*, Dec 2009, pp. 50-56, doi: 10.1109/LAPC.2009.5352587.

2. Nosherwan Shoaib, Sultan Shoaib, Riqza Y. Khattak, Imran Shoaib, and Xiaodong Chen, “MIMO Antennas for Smart 5G Devices,” *IEEE Access*, **6**, Oct 2018, pp. 77014-77021, doi: 10.1109/ACCESS.2018.2876763.

3. Theodore S. Rappaport, Shu Sun ; Rimma Mayzus, Hang Zhao, Yaniv Azar, and Kevin Wang, “Millimeter Wave Mobile Communications for 5G Cellular: It Will Work!,” *IEEE Access*, **1**, May 2013, pp. 335-349, doi: 10.1109/ACCESS.2013.2260813.

4. Qualcomm Technologies Inc. Complicated Relationships. PDF file. November, 2019. https://www.qualcomm.com/media/documents/files/spectrum-for-4g-and-5g.pdf.

5. Mohammad S. Sharawi, Abdelmoniem T. Hassan, and Muhammad U. Khan, “Correlation coefficient calculations for MIMO antenna systems: a comparative study,” *International Journal of Microwave and Wireless Technologies*, **9**, 2, July 2017, pp. 1-14, doi:10.1017/S1759078717000903.

6. S. K. Nikersh, D. Gourab, and G. K. Ravi, “Dual polarized triple-band dielectric resonator based hybrid MIMO antenna for WLAN/WiMAX applications,” *Microw Opt Technol Lett.*, **60**, 5, Mar 2018, pp. 1033-1041, doi: 10.1002/mop.31102.

7. M. S. Sharawi, “Printed Multi-Band MIMO Antenna Systems and Their Performance Metrics,” *IEEE Antennas and propagation Magazine*, Vol. 55, No. 5, pp. 218-232, October 2013.

8. Rakesh N. T., S. Prabhakar, K. K. Binod, and S. Kunal, “Neutralization technique based two and four port high isolation MIMO antennas for UWB communication,” *International Journal of Electronics and Communications*, **110**, 4, Oct 2019, pp. 1-10, doi: 10.1016/j.aeue.2019.152828.